Supplementary Figure 1. p values in negative control series.

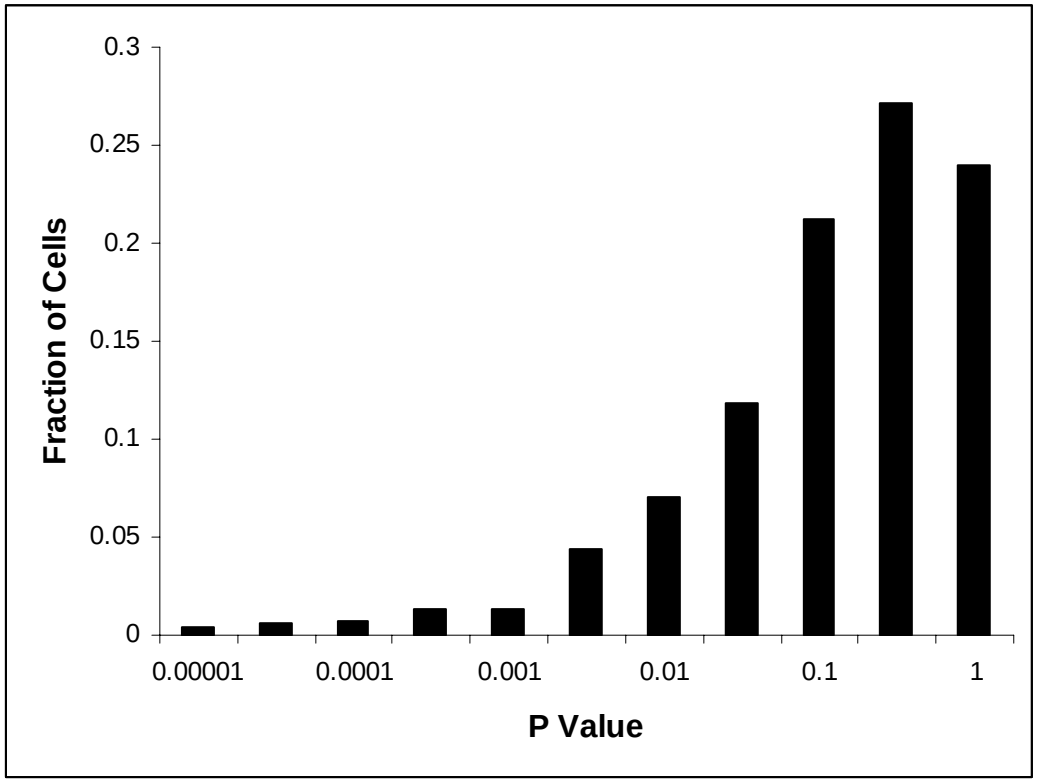

We analyzed two embryos containing no RFP reporter transgene using the same imaging and analysis methods used for the other strains and display histogram of the fraction of cells at each significance level (n = 684). For all cells observed, $P > 3.9 \times 10^{-6}$.

Supplementary Figure 2. Scatter plots comparing red expression for two independent embryos expressing each reporter.

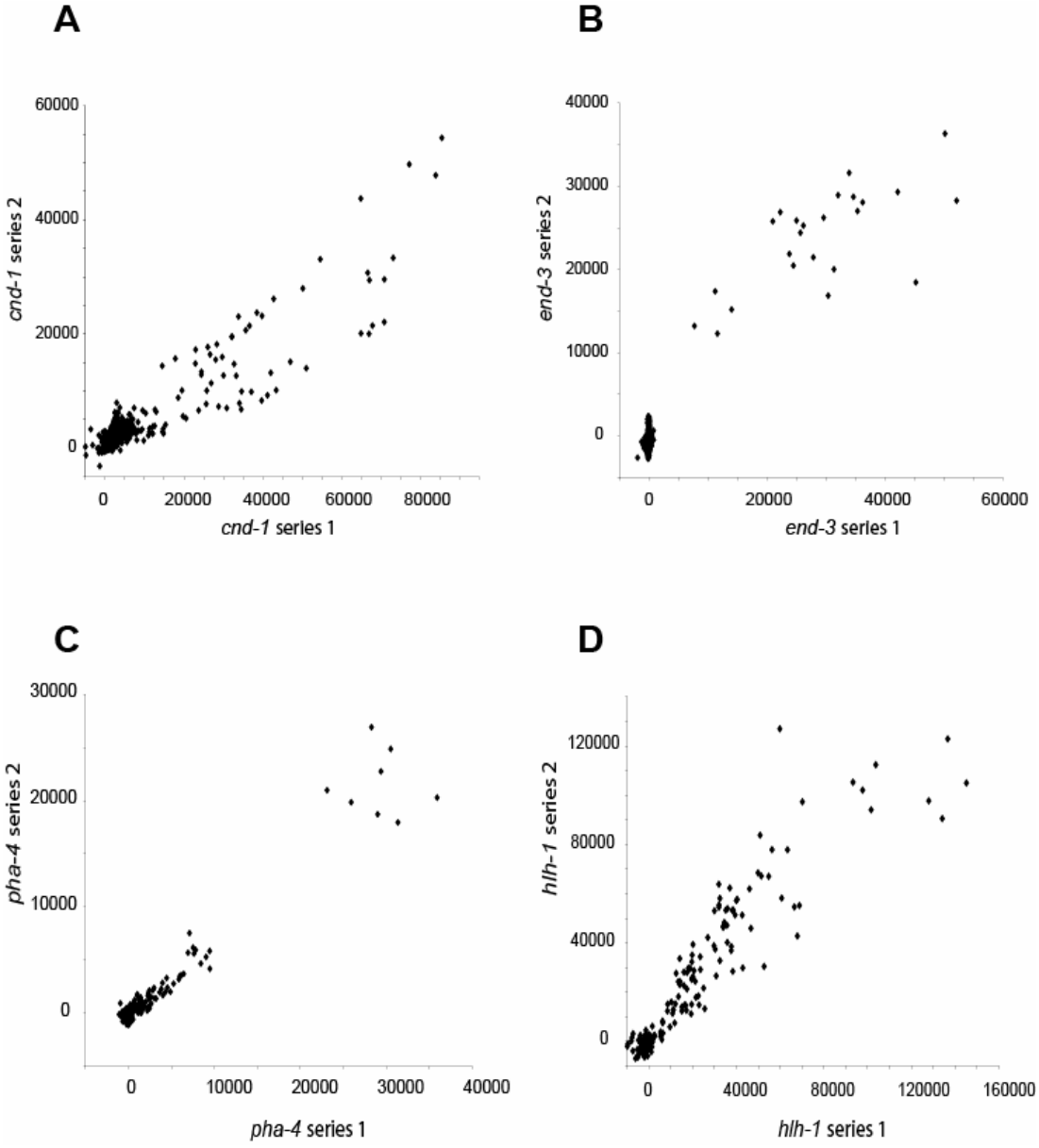

Values plotted are the average expression level for each cell (throughout its lifetime) in the first series (x-axis) and the average expression for the same cell in the second series (y-axis). (**a**) *cnd-1* strain RW10060 (r = 0.92). (**b**) *end-3* strain RW10064 (r = 0.95) (**c**) *pha-4* strain RW10062 (r = 0.97). (**d**) *hlh-1* strain RW10097 (r = 0.94).

Supplementary Figure 3. Graphical display of quantitative reproducibility.

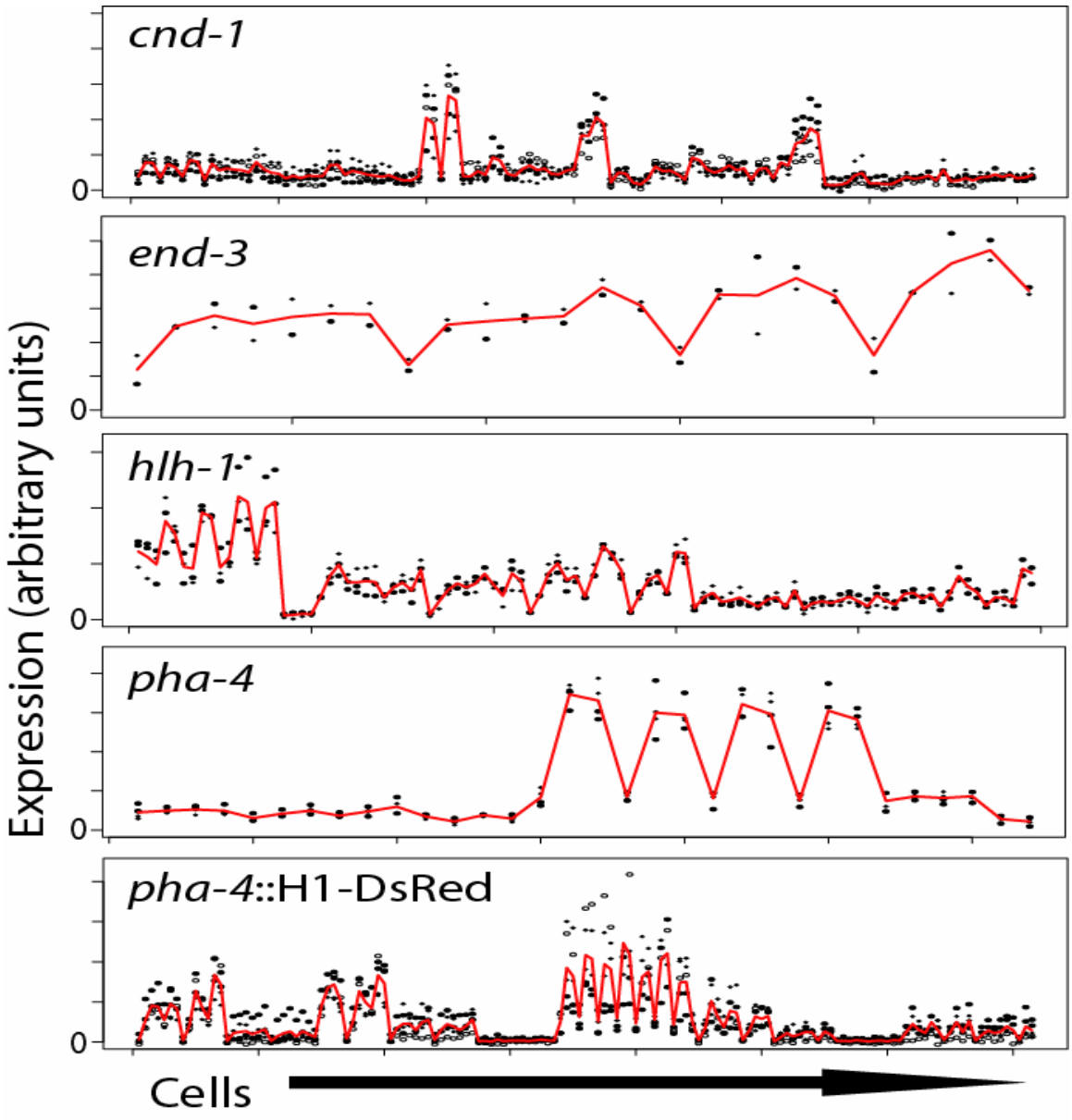

We measured the average expression level in each cell for each embryo. Each panel shows cells (in alphabetical order on the x axis) and their average expression in each replicate series for a given reporter. The red line shows the mean expression for each cell. Each panel contains only the cells passing a one-intensity unit threshold for that reporter gene. The *pha-4*::H1-DsRed reporter is shown separately to demonstrate the higher level of variability seen in that strain.

Supplementary Figure 4. Lineage trees for three different image series for *cnd-1* reporter strains.

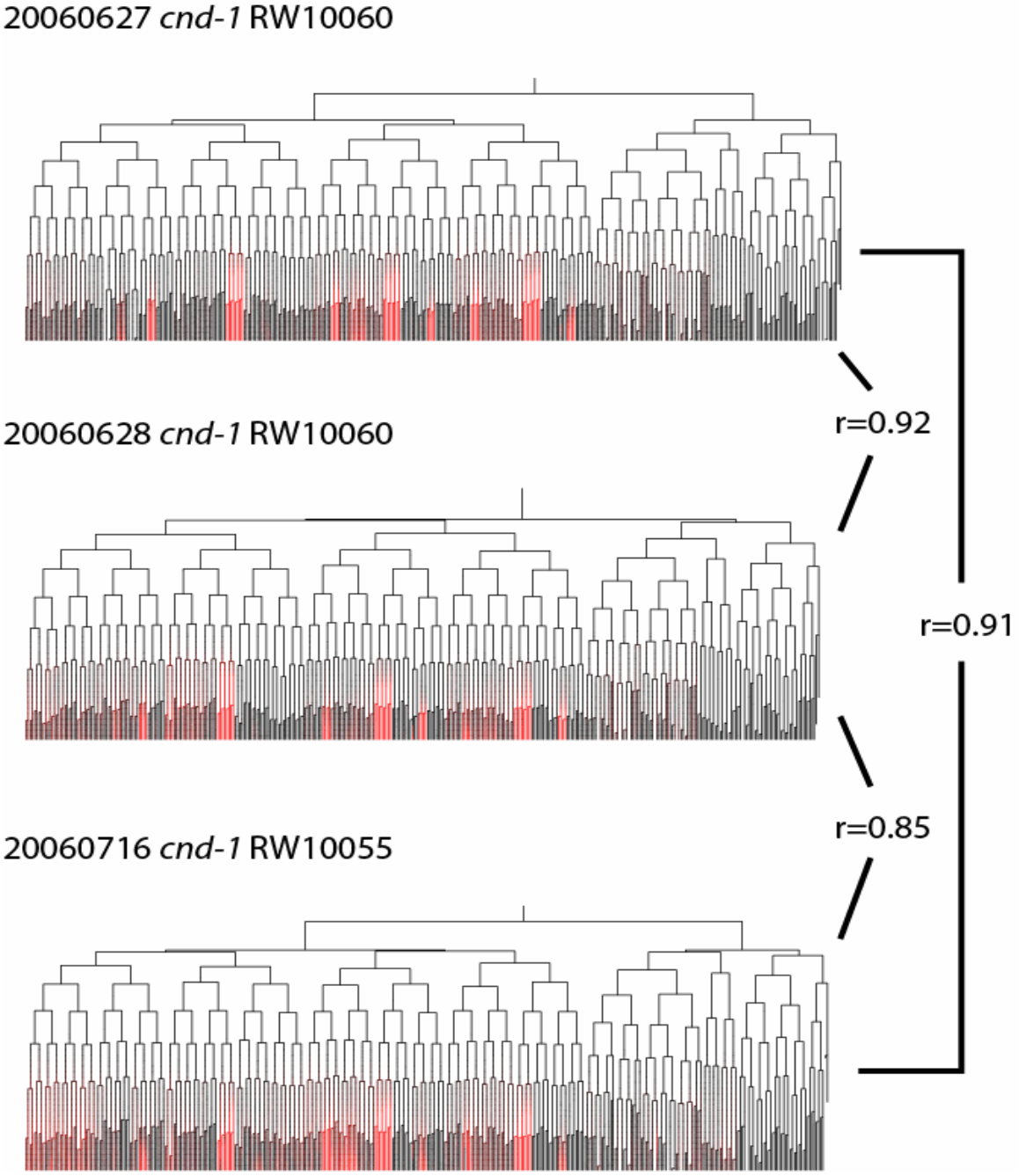

This demonstrates that the identity of brightly-expressing sublineages is the same across embryos and strains for the same *cnd-1* reporter. Correlation coefficients (r) between each pair of series are shown.

Supplementary Figure 5. Confirmation of expression at different significance thresholds.

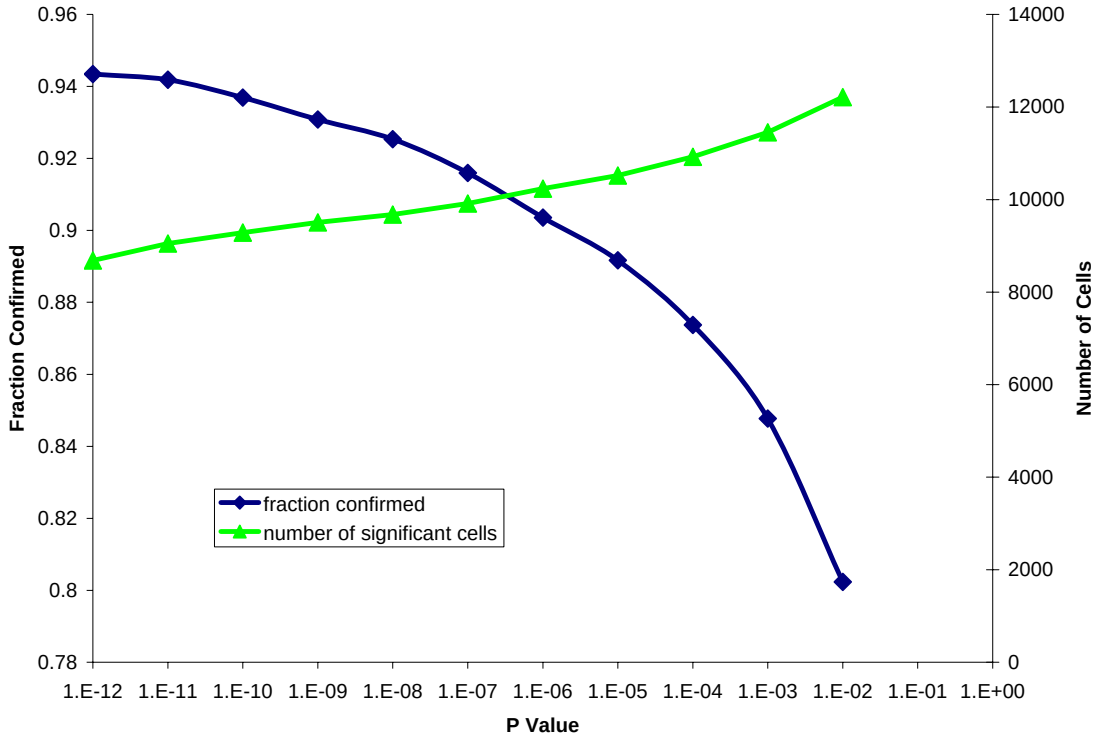

For each pair of embryos containing the same reporter construct, we report the number of terminal cells reaching each significance cutoff in the first embryo (green) and the fraction of those cells with $p < 10^{-6}$ in the second embryo (blue).

Supplementary Figure 6. Consistency of estimated reporter fluorescence onset times in different embryos.

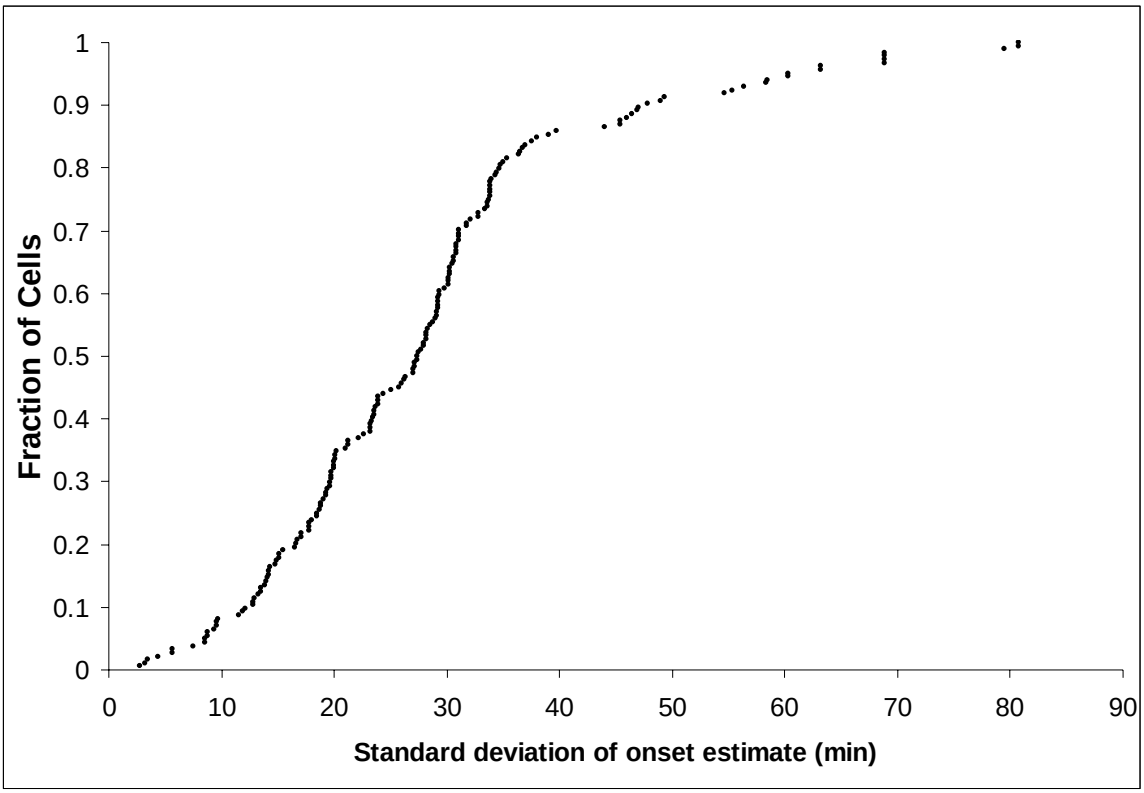

We estimated the time of onset for each expressing cell in each series. For cells identified as expressing in all of the replicate embryos for a given reporter, we calculated the standard deviation of the onset time in minutes (with t = 0 defined as the division time of ABa) and plotted the fraction of unique onset points with a standard deviation below the specified value.

Supplementary Figure 7. Hierarchical clustering of expression patterns

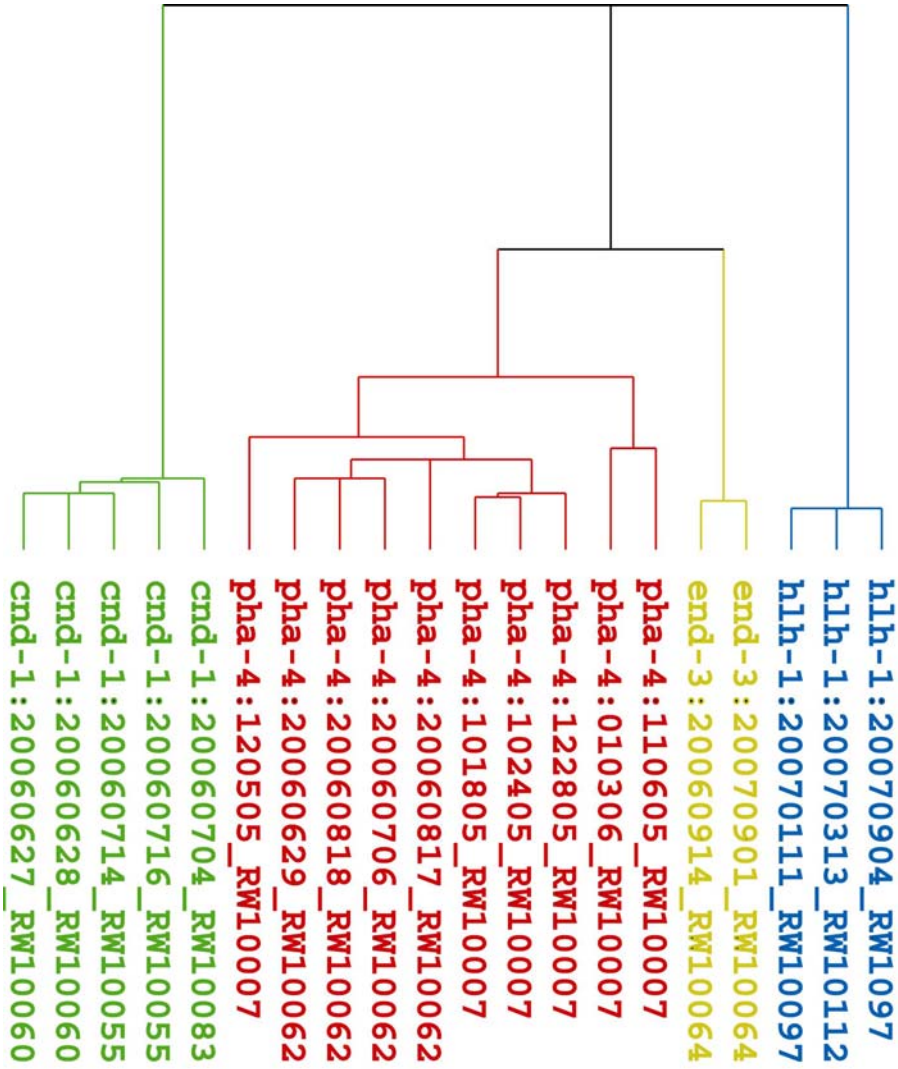

We arranged all of the reported expression by hierarchical clustering. Coloring of branches containing each gene is as in Figure 2.

Supplementary Table 1. Summary of expression pattern reproducibility statistics.

Comparison	Type of comparison	mean correlation (r)	comparisons
end-3::H1-mCherry *vs.* *end-3*::H1-mCherry	Same Strain	0.95	1
cnd-1::H1-mCherry *vs.* *cnd-1*::H1-mCherry	Same Strain	0.92	2
hlh-1::H1-mCherry *vs.* *hlh-1*::H1-mCherry	Same Strain	0.94	1
pha-4::H1-mCherry *vs.* *pha-4*::H1-mCherry	Same Strain	0.96	6
pha-4::H1-DsRed *vs.* *pha-4*::H1-DsRed	Same Strain	0.84	15
cnd-1::H1-mCherry *vs.* *cnd-1*::H1-mCherry	Different Strains	0.86	8
hlh-1::H1-mCherry *vs.* *hlh-1*::H1-mCherry	Different Strains	0.95	1
pha-4 H1-mCherry vs *pha-4*::H1-DsRed	Different Constructs	0.78	24
pha-4 vs. *end-3*	Different Genes	0.68	20
all other comparisons	Different Genes	-0.002	222

Supplementary Table 2. Effect of masking on background-subtracted expression calling

	false positives	false negatives
masked	0	44
unmasked	9	11

Supplementary Methods

Constructs

For most reporters we generated a plasmid *pJIM20* with a multiple cloning site followed by HIS-24 and worm-optimized mCherry[1] coding sequences with a *let-858* 3' UTR and containing a 3.5 kb *unc-119* rescuing sequence. We cloned promoter PCR products anchored adjacent to the native gene's initiator ATG codon for *pha-4* (F38A6.1a(4.1 kb)), *cnd-1*(3.2 kb), *hlh-1*(3.3 kb) and *end-3*(1.0 kb) into this vector. For the *pha-4*-DsRed reporter, we cloned a 4.1kb PCR product from upstream of F38A6.1a into plasmid *pJIM11* containing a HIS-24::DsRed.T1 fusion protein reporter and a *pha-1* rescue fragment. Inserts were confirmed by restriction analysis and sequencing of the junction.

Primer Sequences

Promoter	Left Primer	Right Primer
pha-4	ttagCCCGGGgcccaaattttatgaccaaatga	tagCCTAGGtctcaaattagatagtccttcaaaaa
end-3	ttttCCCGGGtgcaaacttttgactgaaacgaa	ttCCTAGGcatgtttatactttgaatgagaatgcc
hlh-1	ttttCCCGGGtttcagcgagttctcggtctaac	ttttCCTAGGtggaaaattattggaaaatttgga
cnd-1	ttttCCCGGGtcacttgagctcatctcatgctc	ttttGCTAGCtataactggatgacagggaagtg

Restriction sites used for cloning into pJIM20 or pJIM11 indicated in caps.

Strains

Because the original lineaging strain, RW10006, contained the *pie-1*::H2B-GFP allele ruIS32[2], which has a spectrum of tightly linked phenotypes, we used microparticle bombardment with vector pAZ132 to remake this label. This resulted in one integrated line with similar histone H2B-GFP expression in the germline to AZ212 but improved appearance and movement. We mated this line with a strain carrying the integrated *his-72::*GFP transgene *zuIs178*[3] to generate strain RW10029. To allow analysis of strains where the reporter integration site is tightly linked to *zuIS178*, we made an additional strain with the same vector (pSO159) and the same methods as were used previously. This line has similar HIS-72::GFP expression to RW10029 but at a different, unlinked locus (data not shown).

To generate integrated transgenic strains expressing reporter fusions we used microparticle bombardment[2] into either *unc-119(e2498)* or *pha-1(e2123ts)* animals. After three weeks of selection at 25C, we picked animals from independent plates and scored for red expression on a Nikon SMZ1500 fluorescence dissecting scope and a Zeiss Axioplan with a 63x objective. We declared a strain a stable integrant if it generated no *unc-119* mutant progeny for three generations. All markers described here behave as single locus Mendelian traits in crosses. To obtain the strains used for lineage analysis we crossed male RW10029 worms with the Histone-cherry reporter strains, selfed for several

generations and selected homozygous GFP+, mCherry+ progeny for expression analysis. RW10112 (*hlh-1*) and RW10083 (*cnd-1*) were made by crossing them to male RW10026 worms because their RFP transgenes were linked to the HIS-72::GFP transgene in RW10029. The *pha-4::*H1-DsRed strain RW10007 was made using the same methods except with RW10006 as the GFP lineaging marker strain for crossing instead of RW10029. A list of RFP reporter strains used including the number of imaging replicates for each is shown in Table 1.

For the *elt-7* analysis, we crossed *elt-7(ok835)* worms with RW10062(*pha-4*$^{4.1kb}$::HIS-24-mCherry) worms and identified homozygous *elt-7* mutants in the F2 progeny by PCR. For the *lit-1* RNAi experiments, we placed L4 larvae onto plates containing *E. coli* expressing *lit-1* double stranded RNAi [4] (MRC Geneservice, UK) and collected embryos for imaging after 24-72 hours of treatment.

Microscope settings

For the GFP (lineaging) channel, we used the method described previously[9]. For the simultaneous acquisition of mCherry (or DsRed) signal, we used a second track with excitation by a 5 mW 543 nm HeNe laser attenuated linearly between 5% (top plane) and 25% (bottom plane) by the acousto-optical tunable filter, and collected emitted light with a 560-nm long pass filter and PMT with the gain varied linearly between 1100 (top plane) to 1150 (bottom plane), except for strain

RW10062 the laser was attenuated between 8% (top plane) and 40% (bottom plane).

Evaluation of background subtraction methods

We identified significantly expressing cells using each background subtraction method for each *pha-4*::H1-DsRed image series and manually scored cells that deviated between the methods as either false positives or false negatives (Supplemental Table 2). Based on this manual scoring method the unmasked background subtraction method gave a modest false negative rate (6%). In most of these cases, a nearby brightly expressing cell resulted in a high local background signal for a more dimly expressing cell. Masking nuclei before subtraction reduced the false negative rate but caused the appearance of false positives (~2 cells per series) near brightly expressing cells. Because the false negatives were typically identified by examining multiple embryos, we chose the more conservative unmasked strategy.

Tree alignment

For multiple series comparisons requiring alignment to a reference lineage, a single series (102405_pha4red) was selected as the reference series and other series were scaled to match the branch lengths from this series. The scaling was done by interpolating expression values when the number of time points on a branch did not match. To illustrate, imagine a branch in the reference series with 20 time points. If the series being aligned had 19 time points in this branch, the

19 expression measurements would be mapped linearly onto the 20 time points of the reference lineage. For terminal branches, a 1:1 mapping was used.

Residual impact of depth on quantitation

To assess the residual impact of depth on quantification, we compared the difference in expression level for cells in replicate image series with the difference in z plane for four pairs of oppositely-orientated embryos (one pair for each gene). This comparison is simplified because in our mounts, the long axis of the embryo (the anterior-posterior axis) and the dorsal ventral axis are always parallel to the cover slip and the left-right axis perpendicular to it. Embryos rotate to lie only in either of two orientations as has been seen previously[5]. Over the range of depths sampled (~20 micron range), we found an approximately linear effect of depth on intensity with a magnitude of 2.5-3% per plane. This could in theory lead to a maximum 2-fold effect for cells near the cover slip in one series and near the slide in the other. By comparison, ranges in expression levels for significant cells within a given embryo varied by up to 100-fold and frequently by more than 10-fold. Applying a standard correction factor of 3% per plane increased correlation levels modestly (by .03-.05) for comparisons of series of opposite orientation (dorsal-up versus ventral-up), suggesting that it might be possible to further improve quantification with z-correction. Applying this correction to embryos of the same orientation had little or no effect on the correlation. We used the uncorrected values for all subsequent analysis because of the modest effect size compared to the expression differences we observed

and because of the concern that applying a uniform correction might add unanticipated noise to the data. However, the effects of z position bias may need to be considered in cases where very small expression differences are considered for cells that lie in near the top or bottom of the mount either within a series or between series with oppositely oriented embryos.

Equipment and settings

To produce 3D projections of image stacks (Figs. 1a, 3a), we first used the Zeiss LSM510 software to produce a raw projection. We empirically adjusted the various contrast, brightness and opacity controls in this software to produce an image that maximized the detail of individual nuclei and their expression. Colors were converted from red-green to yellow-green by using the “Hue” command in Adobe Photoshop™ to ease interpretation by color-blind readers. The raw images for all recordings are available by request.

1. McNally, K., Audhya, A., Oegema, K. & McNally, F.J. Katanin controls mitotic and meiotic spindle length. *J Cell Biol* **175**, 881-91 (2006).
2. Praitis, V., Casey, E., Collar, D. & Austin, J. Creation of low-copy integrated transgenic lines in Caenorhabditis elegans. *Genetics* **157**, 1217-26 (2001).
3. Ooi, S.L., Priess, J.R. & Henikoff, S. Histone H3.3 variant dynamics in the germline of Caenorhabditis elegans. *PLoS Genet* **2**, e97 (2006).
4. Kamath, R.S. et al. Systematic functional analysis of the Caenorhabditis elegans genome using RNAi. *Nature* **421**, 231-7 (2003).
5. Sulston, J.E., Schierenberg, E., White, J.G. & Thomson, J.N. The embryonic cell lineage of the nematode Caenorhabditis elegans. *Developmental Biology* **100**, 64-119 (1983).